From Tunguska to Chelyabinsk via Jupiter

Natalia A. Artemieva[1,2] and Valery V. Shuvalov[2]

[1]Planetary Science Institute, Tucson, Arizona 85719; email: artemeva@psi.edu

[2]Institute for Dynamics of Geospheres, Russian Academy of Sciences, Moscow 119334, Russian Federation; email: shuvalov@idg.chph.ras.ru

Annu. Rev. Earth Planet. Sci. 2016. 44:37–56

The *Annual Review of Earth and Planetary Sciences* is online at earth.annualreviews.org

This article's doi:
10.1146/annurev-earth-060115-012218

Keywords

airburst, atmosphere, fragmentation, meteoroid, shock waves

Abstract

The Tunguska event remained enigmatic for almost 100 years until the collision of Comet Shoemaker-Levy 9 with Jupiter in 1994 helped to resolve this enigma and allowed us to adequately interpret the more recent Chelyabinsk event. Airbursts typically occur if a meteoroid entering Earth's atmosphere is 10–100 m in diameter, i.e., its energy ranges from 0.5 (Chelyabinsk) to 20 (Tunguska) Mt TNT. All this energy is released in the atmosphere with strong shock waves generated during the entry reaching the surface and causing substantial damage. Atmospheric plumes are capable of dispersing extraterrestrial materials worldwide. Modern civilization is extremely vulnerable to those relatively small disturbances that recur on a decadal timescale and are still difficult to predict.

1. INTRODUCTION

Explosion: this somewhat misleading description of an airburst is often used in popular science publications; although energy release is rapid, neither chemical nor nuclear explosion occurs during entry

Meteorite: extraterrestrial material recovered from the surface, usually >1 mm in size; smaller particles are called micrometeorites and cosmic spherules

On June 30, 1908, a huge explosion ripped through the forests of Siberia. Local newspapers reported the unusual event, which was accompanied by surface shaking, shattered windows, the collapse of a few wooden buildings, thunder-like sounds, and a bright and "hot" light flash from the sky. Seismic disturbances were registered at seismic stations in Siberia, airwaves were detected as far away as England, and magnetic field disturbances with a duration of 4 h were registered in Irkutsk. During the next few days, "white nights" were observed in Europe as far south as Bordeaux. The atmosphere remained more opaque than normal for the whole year, as after a large volcanic eruption. However, there was little scientific curiosity about the impact at the time, possibly due to the isolation of the Tunguska region and the political turmoil of the era, which included World War I, the Russian Revolution, and the Russian Civil War. Without the passionate enthusiasm of the Russian mineralogist Leonid Kulik, it is quite possible that all these observations would never have been connected to an impact event. Kulik was appointed by the Russian Academy of Sciences to search for meteorites in Russia and made numerous discoveries in the European part of Russia. In 1921, he stumbled across a short description of a meteorite fall in Siberia, as observed by passengers on a train, in a tear-off calendar that dated back to 1910. Without any documents describing Kulik's pioneering ideas, we can only speculate that he was familiar with D.M. Barringer's efforts to recover a huge iron meteorite in northern Arizona (Barringer 1909) and with early publications relevant to the subject (Merrill 1908, Öpik 1916, Wegener 1921). Undoubtedly, his main goal was to find meteorites (or an impact crater) in the remote taiga area. It took him 6 years to convince authorities to organize the first scientific expedition, which arrived in the Krasnoyarsk area in 1927 to find not meteorites or impact craters but a huge area of devastated forest with an epicenter at 60°53′09″N and 101°53′40″E (Kulik 1927). The area of the tree fall was almost symmetric about an axis along the 115° azimuth and resembled a triangle or a butterfly. Close to the epicenter, within a distance of 3 km, trees were burned and had branches that were broken and bent toward the surface, but they were still vertical (so-called telegraph poles). Further from the epicenter, trees had fallen mainly radially with minor deviations. During the next expedition, in 1928, some circular depressions with a diameter of ~50 m and a depth of 4–6 m were discovered (Kulik 1938). Concluding his 1938 paper, Kulik wrote,

> We know that on June 30, 1908, behind [the] Podkamennaya Tunguska, an enormous iron meteorite fell. We may imagine that this body broke into pieces, first in the air and then in the Earth's crust, which it penetrated as a number of discrete fragments, and that there (in the crust) these fragments burst into still smaller pieces under the action of the escaping incandescent gases which were produced at the time. We should expect to encounter, at a depth of hardly less than 25 meters, crushed masses of this nickeliferous iron, individual pieces of which may have a weight of one or two hundred metric tons. We estimate that the whole mass of the original iron meteorite, before its encounter with the Earth's atmosphere, was probably as much as several thousands of metric tons, but hardly as much as several tens of thousands. (Kulik 1938, p. 84)

Neither Kulik's expedition nor numerous later expeditions to the site recovered any meteorites. Cosmic spherules found in the 1980s may (or may not) be related to the Tunguska event (Nazarov et al. 1983, Hou et al. 2000).

The butterfly shape of the tree fall was reproduced by Zotkin & Tsikulin (1966) in laboratory experiments that involved detonation of a long explosive cord inclined to the surface at an angle of 30–50° with a spherical charge at its lower end. They argued that the explosive cord produced a cylindrical shock wave equivalent to the ballistic wave created by the meteoroid's entry, whereas the spherical shock wave produced by the spherical charge corresponded to the terminal increase of energy release (i.e., an "explosion") caused by the fragmentation of the meteoroid and the sharp increase in its cross-section. Based on later analysis of available seismic data and the similarity of those data to signals recorded after atmospheric nuclear explosions, Ben-Menahem (1975) estimated the total energy of the event at 9.5–12.5 Mt TNT and the altitude of the terminal explosion at 8.5 km, and Pasechnik (1976) estimated the total energy at 20–50 Mt TNT and the altitude at 2.5–9 km (1 Mt TNT $= 4.184\ 10^{15}$ J). However, another enigmatic problem of Tunguska—the total absence of meteorites—remained unsolved for another 20–25 years. Detailed descriptions of all observations and early studies were summarized by Vasilyev (1998). Nowadays, an impact event accompanied by substantial atmospheric effects but minimal ground effects (and the absence of an impact crater) is referred to as an airburst, in analogy with a military term. Astronomical surveys of near-Earth objects (Harris 2002), detection of bolides in the atmosphere (Brown et al. 2002), and analysis of small fresh craters on the Moon (Werner et al. 2002) allow us to estimate an average time interval between Tunguska-like events on Earth. According to various approaches this timescale ranges from 100 to 10,000 years. Ignoring the fallacy of small-number statistics, one of the key questions during the centennial anniversary of the Tunguska event was, When will the next one occur?

Meteoroid: a cosmic body in the atmosphere, regardless of origin or composition

Fragmentation: a meteoroid's transformation from a single solid body into a swarm of separate pieces under hydrodynamic loading during atmospheric entry

Airburst: rapid transformation of a meteoroid's kinetic energy into thermal and kinetic energy of air during entry; usually related to the meteoroid's fragmentation, vaporization, and deceleration

Near-Earth object: a cosmic body (asteroid or comet) whose perihelion is <1.3 AU

Five years later, the Tunguska event was revived—on a much smaller scale but over a much more densely populated area. Early in the morning on February 15, 2013, thousands of people observed a bright flash in the sky over the city of Chelyabinsk in the Urals region of Russia. The flash was followed by a powerful sonic boom, which shattered windows across an area of $\sim$5,000 km^2, injuring more than 1,500 people, mainly by broken glass. Numerous video recordings of the event have allowed scientists to reconstruct the body's trajectory and fragmentation history with a high degree of accuracy. The entry angle was unusually low, approximately 17° to the horizon; the observed trajectory length in the atmosphere exceeded 250 km. A few flashes occurred between the altitudes of 40 and 20 km. The total mass and energy of the meteoroid were estimated based on its infrasound signal, the energy of the light flash, and ground effects (Brown et al. 2013, Popova et al. 2013). Its preatmospheric diameter was probably around 15–20 m, with a total mass of $\sim 10^7$ kg and a total energy of 300 ± 200 kt TNT ($\sim$1/20 the energy of the Tunguska meteoroid). However, only a small fraction of the meteoroid mass was found near Chelyabinsk—mostly as tiny pieces, with the largest fragment, measuring 600 kg, recovered from Lake Chebarkul. The meteorite is an ordinary LL5 chondrite, the most common meteorite type on Earth. Apart from providing a truly spectacular show, this event was a source of invaluable data that has furthered our scientific understanding of airbursts.

This article presents a review of the current knowledge of atmospheric effects during meteoroid entry, the most recent numerical models describing the Tunguska event, and the application of those models to the Chelyabinsk meteoroid entry. Nonimpact hypotheses and quasi-scientific ideas about the Tunguska "mystery" are not discussed here; curious readers can easily find these speculations elsewhere.

2. PHYSICAL PROCESSES DURING ENTRY

There are three fundamental physical processes involved as meteoroids, the smaller counterparts of asteroids and comets, intersect the atmosphere: deceleration, ablation, and fragmentation. They can be modeled with various degrees of accuracy.

2.1. Simplified Description

Meteor: light flash in the atmosphere accompanying a meteoroid's entry; also known as a bolide or fireball

First, atmospheric drag decelerates meteoroids from their initial velocity (~20 km/s for meteoroids approaching Earth) to a lower limit of free-fall velocity ranging from several centimeters to hundreds of meters per second, depending on the meteoroid size:

$$M\frac{\mathrm{d}V}{\mathrm{d}t} = -C_{\mathrm{d}}\rho_{\mathrm{a}}V^{2}A. \tag{1}$$

In this drag equation M, V, and A are the mass, velocity, and cross-section of the meteoroid, respectively; ρ_a is atmospheric density. The drag coefficient C_d can be calculated by numerical models, measured in experiments, or deduced from observations. In a high-velocity continuum flow, this coefficient depends mainly on the meteoroid's shape and varies between 0.3 and 1.

Second, atmospheric shock waves heat the air surrounding the meteoroid and make it visible as a meteor (also known as a bolide or fireball). Moreover, the thermal radiation produced by shock-heated air evaporates the meteoroid, which may lose more than 95% of its initial mass:

$$Q\frac{\mathrm{d}M}{\mathrm{d}t} = -C_{\mathrm{h}}\rho_{\mathrm{a}}V^{3}A. \tag{2}$$

Here Q is the amount of heat required for vaporization of solid materials (2–10 kJ/g), and C_h is the heat transfer coefficient, which has to be deduced from observations or calculated by methods of radiative hydrodynamics. Typically, its value depends on the altitude, velocity, and size of the meteoroid and varies over a much wider range than the drag coefficient C_d.

Equations 1 and 2 were successfully used in meteoritics to describe bolide phenomena (entry of small, meter-sized bodies) since the 1930s. However, attempts to apply these equations to the Tunguska impact inevitably led to the incorrect conclusion that the meteoroid had a very low density (Petrov & Stulov 1976)—otherwise, the body with a given initial energy reaches the surface with high enough velocity to produce an impact crater. This result, together with the total absence of meteorites and the presence of noctilucent clouds in Earth's atmosphere, was used to advocate a cometary nature for the Tunguska impactor (Petrov & Stulov 1976, Bronshten 1999).

The importance of meteoroid fragmentation was realized much later (Grigorian 1980), and the cometary hypothesis has been seriously questioned since the work of Chyba et al. (1993). The resistance of small meteorites to compression and tension has been measured in laboratory experiments, revealing that their strength is, on average, ~200 MPa, i.e., quite similar to that of terrestrial rocks (Petrovic 2001). At the same time, the best current estimate of the strength of stony meteoroids is in the range of 0.1–1 MPa, as derived from observations of their fragmentation due to dynamic atmospheric loading upon entry (Popova et al. 2011). The most popular explanation of this glaring contradiction is strength degradation with increasing mass, known as Weibull statistics (Weibull 1951). After fragmentation, meteoroids break into smaller, stronger fragments, which in turn are subjected to even higher deceleration and evaporation due to the associated increase in the meteoroid's surface area. There are no simple equations quantifying either the process of fragmentation itself or the motion of the fragmented meteoroid. The pancake model (Chyba et al. 1993, Hills & Goda 1993) treats fragmentation as liquefaction of a solid body and its spreading under hydrodynamic loading in the direction perpendicular to the trajectory; i.e., its radius R (and hence the cross-section A in Equations 1 and 2) is not a constant value after fragmentation:

$$R\frac{\mathrm{d}^{2}R}{\mathrm{d}t^{2}} = \frac{C_{\mathrm{d}}\rho_{\mathrm{a}}V^{2}}{\rho_{\mathrm{m}}}, \tag{3}$$

where ρ_m is the meteoroid density. Importantly, in this model, the fragmented meteoroid is still treated as a continuum with constant density. In contrast, the separated fragments model (Passey & Melosh 1980, Artemieva & Shuvalov 2001) assumes that fragmentation divides the body into discrete fragments with a lateral separation velocity U given by

$$U = V\sqrt{C_1 \frac{\rho_a}{\rho_m}}, \tag{4}$$

where C_1 is the coefficient of an order of 1, which can be calculated (Artemieva & Shuvalov 2001) or estimated from observations (Passey & Melosh 1980). Then each fragment is treated as an independent body, which decelerates and ablates according to Equations 1 and 2. In both models the expansion of the fragment cloud leads to an "explosive" energy release in the atmosphere. Each model is an oversimplified description of a complex process (Svetsov et al. 1995); the pancake model is more suitable for large, weak bodies (stony meteoroids and comets), whereas the separated fragments model is better suited to the study of terrestrial crater-strewn fields created by fragmented iron meteoroids (Artemieva & Shuvalov 2001). The most advanced models combine both approaches: Some fragments are treated as clouds of dust subjected to pancaking and some as separated fragments (Borovička et al. 2007, 2013; Popova et al. 2013).

2.2. Full-Scale Hydrodynamic Description

The simplified approach (Equations 1–4) describes the trajectories and final masses (meteorites on the surface) of meteoroids entering the atmosphere if drag and ablation coefficients are known from more sophisticated models, observations, or experiments. However, this approach does not describe the propagation of atmospheric shock waves created by hypersonic flight, the interaction of shock waves with the surface, and other impact-related events. To address these problems, full-scale hydrodynamic modeling (i.e., solution of the Euler equations for mass, momentum, and energy conservation) with radiative transfer must be used. Fortunately, the entry problem can be restricted to two dimensions if the meteoroid is much smaller than the atmospheric scale height (∼8 km on Earth) and has a simple axisymmetric shape. Unfortunately, calculations of the entry process of small meteoroids (<10 m in diameter) are problematic for a few reasons. First, individual (and unknown) properties of these meteoroids (such as shape, strength, presence of cracks, dust content, and ablation rate) can dominate their behavior during entry. Second, the accuracy of hydrocode calculations depends on resolution [number of computational cells per impactor radius (Pierazzo et al. 1997)], so the trajectory length of small meteoroids measured in impactor radii is much longer than for larger meteoroids and requires much more computational time. Thus, simplified Equations 1–4 are still a more efficient approach to fit the model to observed data (light curves, trajectories) for typical meteoroid scenarios. The Chelyabinsk event belongs exactly to this class of events; although hydrodynamic modeling is theoretically possible, it is not efficient and does not reproduce peculiarities of the observed light curve. On the contrary, larger Tunguska-like bodies are more suitable for hydrodynamic modeling: Although their strength is lower, they penetrate deeper into the atmosphere and experience greater dynamic loading and hence stronger fragmentation; intense melting and vaporization further facilitate their liquid-like behavior. At this scale, the unique properties of individual objects are not of crucial importance (Svetsov et al. 1995).

There are many hydrocodes that can deal with airburst problems. In the following sections we focus on the results obtained by the Eulerian shock-physics hydrocodes CTH (McGlaun et al. 1990) and SOVA (Shuvalov 1999b). Both codes can model multidimensional (1D–3D), multimaterial (3–10 materials with different thermodynamic and constitutive properties), large-deformation gasdynamic flows. Radiative heat transfer may be also taken into account in a simplified manner. There is one important difference between the CTH and SOVA approaches to the airburst problem. The former describes penetration without ablation in a pure hydrodynamic regime and prescribes an additional explosion (i.e., internal energy release) to correctly reproduce energy deposition in the atmosphere (Boslough & Crawford 1997, 2008). The latter includes ablation and is able to reproduce the terminal explosion without an artificial energy release (Artemieva & Shuvalov 2007, Shuvalov & Trubetskaya 2007). Certainly, this is a more physically correct approach. However, the introduction of an explosion simplifies calculations dramatically by removing the need to solve the radiation transfer equations and by allowing the simulation to begin with the meteoroid at a lower altitude, closer to the altitude of peak energy release.

3. MODELING THE TUNGUSKA EVENT

3.1. Early Models: 1970s to 1980s

The first numerical models of the Tunguska event were published in the 1980s, mainly in Russian. Korobeinikov et al. (1998) provided a good summary of these research efforts. Inevitably, due to computational limits, these models described the Tunguska event as a point source (spherical 1D problem) or an elongated source (cylindrical 2D problem) explosion. The best results were obtained in late 1980s when these two kinds of explosion were combined in analogy with experiments (Zotkin & Tsikulin 1966) and the interaction of the resulting shock waves with the surface was taken into account. These calculations made use of seismic records, barograms, and measurements of fallen trees and were calibrated with nuclear airburst data. The complex approach to the Tunguska entry problem (Korobeinikov et al. 1998) includes the following steps:

1. The entry is analytically modeled (see Section 2.1, Equations 1 and 2), with drag and heat transfer coefficients calculated separately from the full system of radiative gasdynamics (Chushkin & Sharipov 1990).
2. Thermoelastic stresses within a homogeneous spherical body during the entry are calculated, and the body's fracturing and fragmentation are estimated. The results from step 1 (temperature and pressure) are used as boundary conditions.
3. The deceleration of the totally fragmented body (a mixture of solid fragments, melt droplets, vapor, and hot atmospheric gas) is described by introducing an additional energy release immediately after the fragmentation, when the cloud still has high velocity along the trajectory. The potential source of this excessive energy is not clear. The authors suggest that it could be the combustion energy of volatiles and/or carbon released during fracturing as well as the recombination of hot vapor into molecules. Next, the motion of a gaseous jet is described by using the gasdynamic approach. After the explosion, the jet expands laterally and loses its velocity quite quickly, traveling just a few kilometers along the trajectory before the final stop. The altitude of the explosion and the amount of added energy are free parameters that must be determined by matching modeling results with observations. Interestingly, Boslough & Crawford (2008) used a similar concept of an additional explosion to model the Tunguska event using the CTH hydrocode.
4. The interaction of shock waves generated in the atmosphere (step 3) with the surface requires, strictly speaking, a 3D approach. However, the authors manage to find a quasi-analytical solution of shock waves' reflection from the surface and treat the maximum pressure (the sum of thermal pressure and dynamic pressure, which is dependent on the horizontal component of gas velocity) at any point on the surface immediately after the reflection as a destructive factor.

Korobeinikov et al. (1998) found that the best correlation with observations occurs if the total energy of the Tunguska body is approximately 20 Mt TNT (5–25% of this energy is artificially released during the explosive step 3) and the entry angle is 40° to the horizon. Then they returned to step 1 to deduce the Tunguska impactor's entry parameters and the altitude of the explosion. The authors found that both icy and stone bodies with velocities as low as 11.2 km/s and up to 35 km/s could produce the observed physical phenomena. Finally, they suggested two most likely scenarios for the Tunguska event: (*a*) a fragment of a comet nucleus with a density of 0.5–0.6 g/cm^3, a velocity of 33–37 km/s, and a radius of 40 m or (*b*) a large carbonaceous chondrite with 5–10% water content, a density of 2 g/cm^3, a velocity of 26 km/s, and a radius of 30 m.

Comet Shoemaker-Levy 9: a string of this comet's fragments collided with Jupiter in 1994 at 60 km/s with observed effects similar to those expected for terrestrial airbursts

3.2. Comet Collision with Jupiter and a New Era in Airburst Models

Whereas the study of impact cratering blossomed after the breathtaking discovery that the Cretaceous–Paleogene mass extinction was connected with an asteroid impact (Alvarez et al. 1980), much smaller (and much more frequent) airburst events were mainly forgotten. This situation changed dramatically after the discovery in 1993 of the impending collision of Comet Shoemaker-Levy 9 and Jupiter in 1994 (Shoemaker et al. 1993). It was predicted that the penetration stage would occur on the dark side of Jupiter and hence would be observed only by *Galileo* instruments (Carlson et al. 1995) and the *Hubble Space Telescope* (Weaver et al. 1995). However, preliminary estimates showed that a fireball produced by impactor explosion could rise above the limb and thus could be directly observed by Earth-based telescopes. Thus, prior to impact, computational efforts were focused on making predictions to help astronomers observe the event as fully as possible. Modelers were able to take advantage of this dramatic validation experiment to improve their physical models and computer capabilities and to revive interest in these much less powerful but much more frequent events, which include the Tunguska airburst.

3.3. Penetration Models

Crawford et al. (1994) used the CTH shock-physics code to simulate the penetration of cometary fragments 1–3 km in diameter with Jupiter. During penetration, the impactor transfers its kinetic energy into the thermal energy of the comet, serving to heat and evaporate it, and into the kinetic and thermal energy of Jupiter's atmosphere, producing an impact flash. The amplitude and duration of these flashes were later compared with *Galileo* observations to estimate Shoemaker-Levy 9 fragment sizes (Boslough et al. 1994, Crawford 1997, Nemtchinov et al. 1997). Modeling of penetration revealed that (*a*) disruption and total evaporation of the comet occur at high velocity, close to the pre-entry velocity, and (*b*) the impactor decelerates only after its total evaporation and transformation into a gaseous jet. Similar models can be applied to the scenario of much smaller Tunguska-like bodies entering Earth's much thinner atmosphere (Boslough & Crawford 1997, Shuvalov & Artemieva 2002, Shuvalov & Trubetskaya 2007). **Figure 1*a*** shows the initial stage of the entry: At an altitude of 30 km, the body loses its integrity and starts to deform by widening in the direction perpendicular to its trajectory (pancaking). This widening is accompanied by the growth of Rayleigh-Taylor and Kelvin-Helmholtz instabilities. At an altitude of 20 km (**Figure 1*b***), the body's radius has doubled, the shape is strongly disturbed, and the impactor is on the verge of total disintegration. Between the altitudes of 20 and 16 km (**Figure 1*c***), small fragments still move at high velocities and are quickly transformed into a gaseous jet, a mixture of tiny fragments (not visible in the figure), melt droplets, and vapor. Below this altitude, the jet decelerates, and by ~6 km in altitude it has totally lost its momentum. The jet remains rarefied with a density 1–2 orders of magnitude lower than the ambient air density; the temperature of the vapor-air mixture is several thousand degrees (**Figure 1*d***). The results of this 2D entry model are interpolated onto a 3D mesh model to simulate either the interaction of shock waves with the surface or plume evolution (Artemieva & Shuvalov 2007).

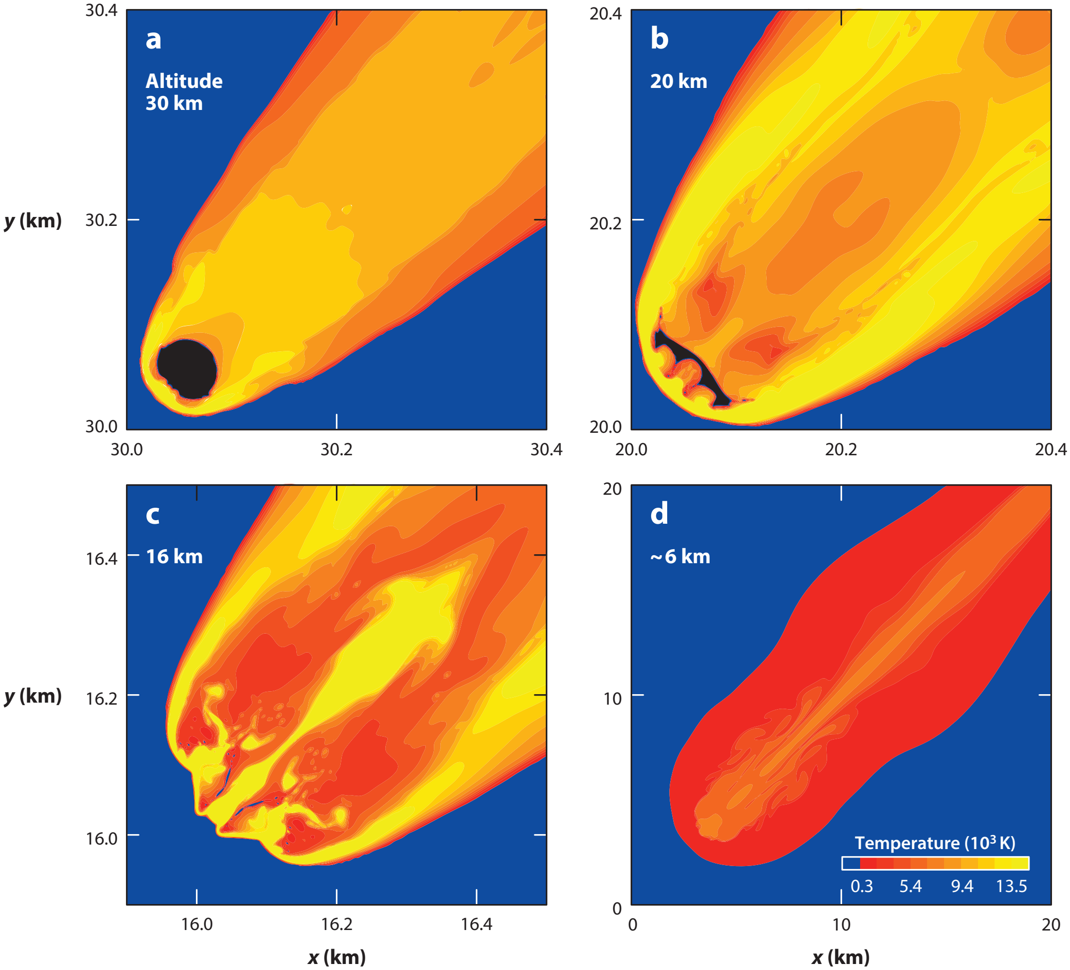

Figure 1

Snapshots showing temperature distribution during the entry of a Tunguska-like body. (*a*) At an altitude of 30 km, fragmentation begins. (*b*) At an altitude of 20 km, the body is totally fragmented and has a pancake shape. (*c*) At an altitude of 16 km, the body is transformed into a jet of particles, although the velocity is only slightly lower than the entry velocity. (*d*) At the deepest penetration of the jet, its velocity drops to zero (the spatial scale is different from that in panels *a–c*).

3.4. Ground Effects: Pressure Pulse, Stormy Winds, and Fires

Shock waves generated during meteoroid entry continue to propagate downward and may reach the surface within seconds or minutes, depending on the altitude of the airburst. When these aerial blast waves reach the ground, they generate Rayleigh seismic surface waves and earthquakes. If the pressure on the ground is known as a function of coordinates and time, the energy of the seismic waves can be calculated using a solution of Lamb's problem (the response of an elastic half-space to a vertical load) and calibrated against published nuclear test data. Svettsov (2007) obtained earthquake magnitudes from 4.8 to 5.0, assuming that the energy of the Tunguska event was between 7 and 18 Mt TNT. **Figure 2*a*** shows distributions of the maximum pressure for a 45° impact releasing energy equivalent to 10 Mt TNT (Artemieva & Shuvalov 2007). The maximum

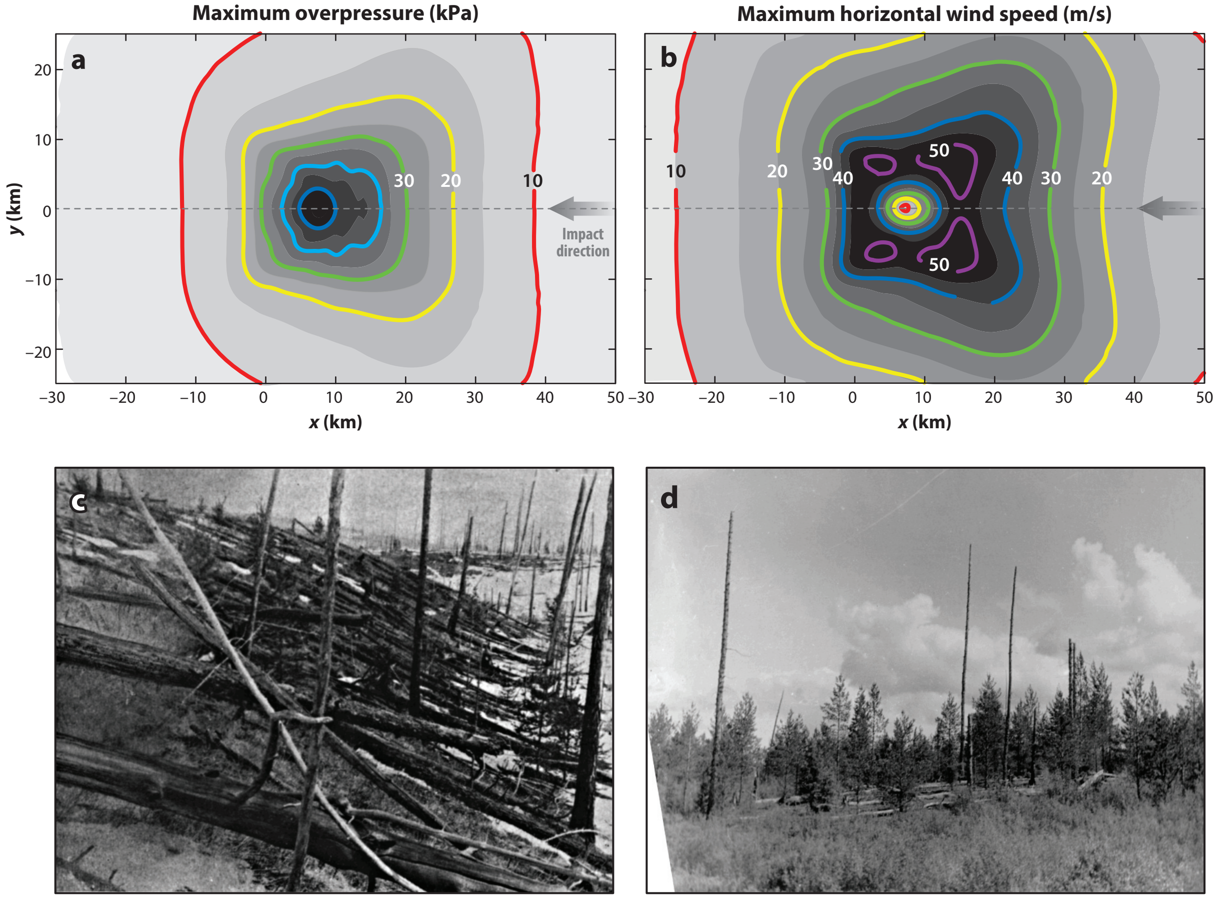

Figure 2

(*a*) Maximum overpressure on the surface and (*b*) maximum horizontal wind speed after a Tunguska-like impact with 10 Mt TNT total energy. The impactor comes from the right along the *x* axis. (*c*) The forest between the two blue contours in panel *b* (wind speed >40 m/s) is totally damaged, as seen here in Kulik's photograph of the Tunguska site. The yellow contour (wind speed >20 m/s) restricts the devastated area. (*d*) So-called telegraph pole trees occur near the point where $x = 8$ and $y = 0$ in panel *b* (wind speed <20 m/s), as seen here in Plekhanov's photograph of the Tunguska site.

pressure exceeds standard atmospheric pressure by 50% within a 5-km-diameter area and remains high enough (10% above standard) to cause damage within a 50-km-diameter area. In addition, the interaction of bow shock waves with the surface results in airflow along the surface (stormy winds), which slowly decays at distances of 20–30 km from ground zero in the case of the Tunguska event (**Figure 2*b***). Observations of nuclear weapon tests in the early 1960s (Glasstone & Dolan 1977) can be used to estimate the wind speed values responsible for tree damage: Minimal damage occurs at wind speeds below 25 m/s, moderate damage (30%) at wind speeds of 40–45 m/s, and severe damage (90%) at wind speeds exceeding 55–65 m/s (for comparison, the maximum hurricane wind speed is ~70 m/s). Interestingly, in the epicenter, the wind speed is very low, because the shock waves approach the surface vertically. This area corresponds to the area around the Tunguska impact where Kulik observed trees that resembled telegraph poles, standing upright with all their branches bent down and burned (it is also the area with maximum radiation flux to the surface).

Boslough & Crawford (1997) presented similar distributions of winds near the surface after an explosion with 12 Mt TNT total energy. They claimed that the total energy of the Tunguska body could be as low as 3–5 Mt TNT and still produce similar ground effects for the following reasons: (*a*) The penetration jet has more momentum toward the surface than a point explosion does, and hence nuclear test results cannot be directly used; (*b*) the local forest in Siberia was not healthy and would have been damaged at much lower winds/pressures than those derived from nuclear tests; and (*c*) topography, such as ridges, would have enhanced dynamic pressures locally. Although the latter effect was reproduced numerically (Boslough & Crawford 2008), it probably leads to a less homogeneous distribution of disturbances than that given by flat-surface models; that is, both local decreases and increases of maximum overpressure and wind speed occur.

The taiga area subjected to the 1908 fire had a shape similar to the area of flattened trees and was half its size (i.e., 15–20 km in diameter and up to 25–30 km in the southeast direction along the bolide trajectory (Vasilyev 1998). Analysis of fire consequences showed that the fire started immediately within a large area but was rather weak (only dry trees were ignited) and did not propagate far due to a high groundwater level. Radiation emitted by hot air and vapor during entry of the Tunguska body (**Figure 1**) was the main source of heat to the surface. Numerical simulations (Svetsov 1996, 1998) have shown that the total radiation on the surface at a distance of 15 km from the epicenter is released within 10 s and varies between 350 and 700 kJ/m^2 for clear and very clear atmospheric conditions, respectively. These values are close to the critical energies required to ignite dead leaves (350 kJ/m^2) and even pine needles (900 kJ/m^2) as defined in nuclear explosion tests (Glasstone & Dolan 1977).

3.5. Plume Evolution in the Atmosphere: Impactor Fate, White Nights, and Geomagnetic Disturbances

Simulation results of the Shoemaker-Levy 9 plume (Crawford et al. 1994, Zahnle & MacLow 1994) indicated that early fireball growth is predominantly directed outward along the incoming bolide trajectory but is later redirected toward growth dominated by the vertical gradient of the Jovian atmosphere (**Figure 3*a***). Numerical predictions were in excellent agreement with observed fireballs (Hammel et al. 1995). Although the expectations were based on analogy between an airburst and a nuclear explosion, the model revealed that atmospheric plumes are fundamentally different from fireballs produced by nuclear explosions, in which the buoyant plume is formed as a result of air and device heating by emitted radiation and shock compression, rises vertically, and is then transformed into a mushroom cloud. In the Shoemaker-Levy case (and all other meteoroid airbursts), the total kinetic energy of the impactor is deposited directly in an atmospheric wake, and the mixture of atmospheric gases and impactor materials expands outward and accelerates upward along the atmospheric wake due to the absence of hydrostatic equilibrium.

To determine the fate of the Tunguska impactor, Artemieva & Shuvalov (2010) transformed the impactor vapor (**Figure 1*d***) into a collection of tiny particles—chilled melt or vapor condensates—and used multiphase hydrodynamics (Shuvalov 1999b) to follow their evolution in the atmosphere. The mixture of these particles with hot air is buoyant and quickly moves upward along the rarified wake, forming a plume (**Figure 3*b***) very similar to the Shoemaker-Levy 9 plume (**Figure 3*a***). Although at high altitudes the mixture density exceeds the local atmospheric density, the mixture continues to rise owing to its inertia and gradually loses momentum to gravity. After three minutes, the cloud reaches an altitude of 400 km and is almost spherical. Two distinct parts of the plume can be identified—a narrow stem below the altitude of 80 km is crowned by a huge cap. The stem particles precipitate slowly according to Stokes' law, are dispersed by local winds, and are deposited within a few hundred kilometers from the impact site (Artemieva & Shuvalov 2010). It is likely that

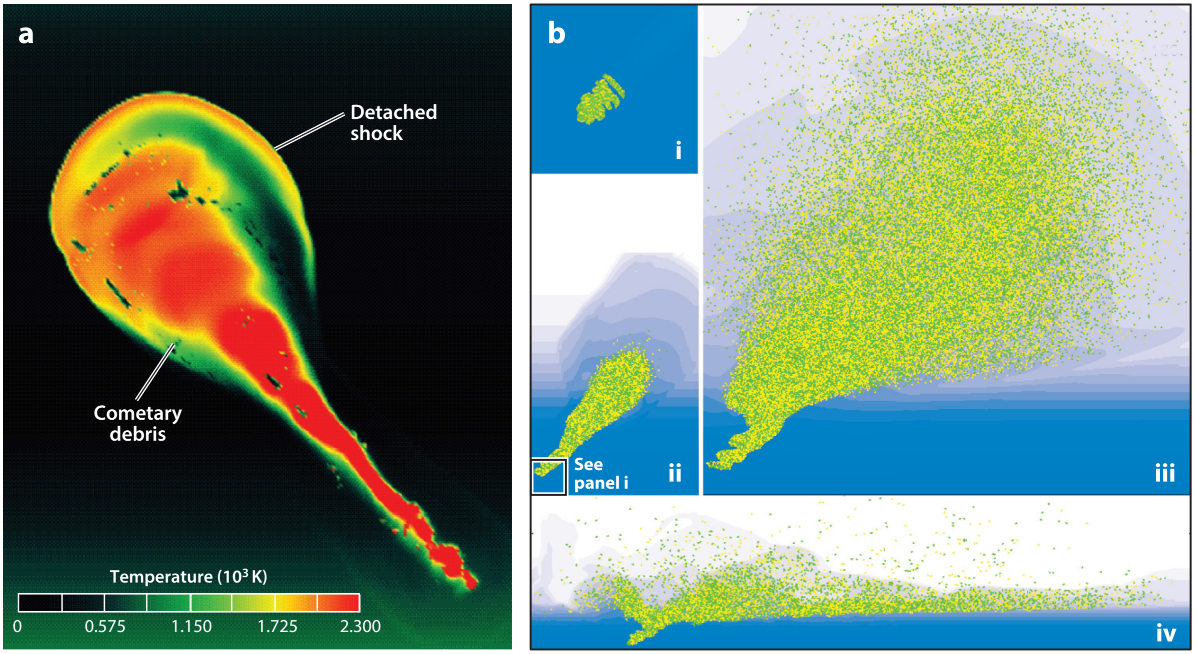

Figure 3

(*a*) The plume formed 1 min after the collision of Comet Shoemaker-Levy 9 with Jupiter. Image courtesy of David Crawford. (*b*) Plume evolution after the Tunguska impact (Artemieva & Shuvalov 2010). The atmosphere is shown in blue and the impactor particles in green (10 μm in radius) and yellow (1 μm in radius). (*i*) Total deceleration of the impactor; particles are produced. The frame is 20 × 20 km (compare with **Figure 1*d***). (*ii*) One and (*iii*) three minutes later; the small square in the bottom left corner of panel *ii* corresponds to panel *i*. The frame size is 400 × 400 km. (*iv*) Ten minutes later; the plume collapses. The frame size is 1,500 km × 400 km.

all extraterrestrial contaminations found in Siberia so far (Nazarov et al. 1983, Hou et al. 2000) are related to the presence of these particles. The plume containing cap particles collapses under gravity, initiates strong atmospheric flows in the thermosphere, and spreads out to a distance of 2,000 km within half an hour. Similar effects were observed (but not modeled) on Jupiter during the collapse of cometary impact plumes (Hammel et al. 1995). Late evolution of these particles is defined by global atmospheric circulation at high altitudes. Assuming worldwide distribution of the cap particles, the average concentration of extraterrestrial material on the surface may be approximately 0.03 kg/km^2. Even if the cloud is diffused exclusively within the polar region of the Northern Hemisphere, the concentration is still low—comparable to the annual flux of cosmic dust onto Earth (0.1 kg/km^2).

The hydrodynamic models described above have shown that, at the end of the penetration stage, a solid body the size of the Tunguska body is transformed into a mixture of vapor with molten particles that later evolve within the plume and are dispersed over a large area. However, this scenario is not quite correct, as these models treat the meteoroid as a continuum; that is, they neglect the production of sizeable solid pieces during fragmentation. Such fragments are routinely observed (and some of them later recovered) during large meteorite falls (e.g., Popova et al. 2011). On the contrary, not one Tunguska meteorite has been found so far, despite numerous expeditions to the site. What happened to these surviving fragments after the Tunguska fall? Were they separated from the main jet to land as meteorites and lost forever in local swamps? Or were they never formed because of a specific entry scenario (e.g., all materials were vaporized rather than fragmenting into sizeable pieces)? Although we cannot exclude the latter, it seems that a meteorite search in this area is very unlikely to be successful. Svetsov (1996, 1998) showed that relatively small (<10 cm) fragments produced during terminal fragmentation are subjected to extremely strong radiation independent of their position (inside or outside of the fireball) and are completely evaporated within a few seconds. Larger (>10 cm) fragments could survive, but their mass fraction would probably be very low (if not zero), and the chances of finding such fragments in dense tundra are minimal.

Polar mesospheric clouds (PMCs): clouds consisting of tiny ice crystals, concentrated at an altitude of ~82 km and typically observed during summer at 50–65° latitude

International Monitoring System: a worldwide observational network that helps verify compliance with and detect and confirm violations of the Comprehensive Nuclear Test-Ban Treaty

The plume not only carries the fine impactor materials away from the impact site but also lifts tropospheric water into the mesosphere, which is normally extremely cold and dry. Three minutes after the explosion, the mass of mesospheric water vapor reaches 15–20 kt, and it remains rather large for a long time period (Artemieva & Shuvalov 2010). This means that the mesospheric cloud (**Figure 3*b***, panel *iv*) is oversaturated with water vapor; that is, it is at least an order of magnitude more water rich than a standard polar mesospheric cloud (PMC) with 20–200 μg/m^2 of water (Thomas & McKay 1985), and thus the plume could be an order of magnitude brighter. The presence of impactor particles promotes the growth of ice crystals. Further evolution of this cloud is driven by mesospheric winds. It has been observed that space shuttle exhaust releasing ~300 t of water at altitudes above 100 km produces a PMC (Stevens et al. 2003, Kelley et al. 2009). These so-called technogenic PMCs originate in Florida, reach the polar region within one day, and are subsequently visible for about a week. It is possible that the Tunguska cloud reached northern Europe within ~20 h, creating an extremely bright PMC and hence producing white nights at low latitudes.

Finally, the collapsing plume generates perceptible oscillations in the upper atmosphere. These oscillations cause disturbances of the E layer in the ionosphere and can be registered by magnetographs at large distances. As the pattern of geomagnetic disturbances depends on the Tunguska entry azimuth, comparison of calculated and observed disturbances can be used to estimate this azimuth independently from previously used methods (Kovalev et al. 2006, Kuzmicheva & Losseva 2012).

4. MODELING THE CHELYABINSK EVENT

Concluding their comprehensive review, Boslough & Crawford (1997, p. 278) wrote, "There is a high probability that another plume-forming impact will take place on Earth within our own lifetimes. The next such event should be anticipated as potential hazard, but also as an opportunity to gather more information on the physics of atmospheric entry, ballistic fireball growth, and plume collapse." This event did occur 16 years later, just 2,400 km southwest of the Tunguska site. Although, strictly speaking, the Chelyabinsk entry was not a plume-forming impact, its energy was high enough to cause substantial drama on the surface, to attract public attention worldwide, and to allow us to apply some of the Tunguska models to this dramatic event. Thanks to global detection systems (geostationary satellites and the International Monitoring System) and especially to widely available electronic gadgets (dashboard cameras, cell phones, and security cameras), it is the best-characterized airburst to date. A summary of all observations and their detailed analysis may be found in the supplementary materials provided by Popova et al. (2013).

4.1. Entry Model and Ground Effects

Meteoroid fragmentation began at an altitude of 83 km, with peak radiation occurring at an altitude of ~30 km and a velocity of 18.6 km/s (Brown et al. 2013, Popova et al. 2013). The light curve was reconstructed by careful calibration of all available observations. Analysis of numerous videos also made it possible to extract trajectories of some individual fragments (Borovička et al. 2013). All collected information was used in the hybrid fragmentation model (Equations 1–4) to estimate the entry mass and to predict final masses and positions of meteorites on the surface. Although the solution of these equations is not unique (e.g., another set of fragment sizes could produce similar light curves), the landing site of the largest fragment was predicted with an accuracy of a few hundred meters (Borovička et al. 2013). Full-scale modeling of meteoroid penetration is unlikely to be successful, as explained above (Section 2.2), as the entry dynamics are controlled by specific properties of the meteoroid that in general will not be captured in a single set of pure hydrodynamic simulations.

To model the shock waves produced by the Chelyabinsk entry and the evolution of its smoke train in the atmosphere, the complex penetration process can be mimicked by a series of cylindrical explosions distributed along the entry trajectory according to the observed energy release in atmosphere (Crawford et al. 1994, Brown et al. 2013, Popova et al. 2013, Artemieva & Shuvalov 2014). Estimates of the total released energy vary from 100 to 500 kt TNT. Shock waves generated by these explosions decay quite quickly, so the moment of shock wave arrival at any point on the ground does not depend on the position of the main flash along the trajectory: Sound arrives at a given location from the nearest point along the meteoroid's trajectory. Calculated overpressure contours of $\Delta p > 0.5$ kPa and $\Delta p > 1$ kPa are shown in **Figure 4*b***. This pattern correlates well with the observed area of broken windows. The damaged area is elongated in the direction perpendicular to the trajectory in a manner that is similar to the Tunguska butterfly (**Figure 4*a***) but not identical (because of the difference in total released energy, entry angle, and altitude of maximum energy release). The calculated magnitude of the seismic source is 3.85 and 4.0 for a total energy of 300 and 500 kt TNT, respectively. These values are in reasonable agreement with registered seismic waves. The earthquake magnitude of the Chelyabinsk event corresponds to a

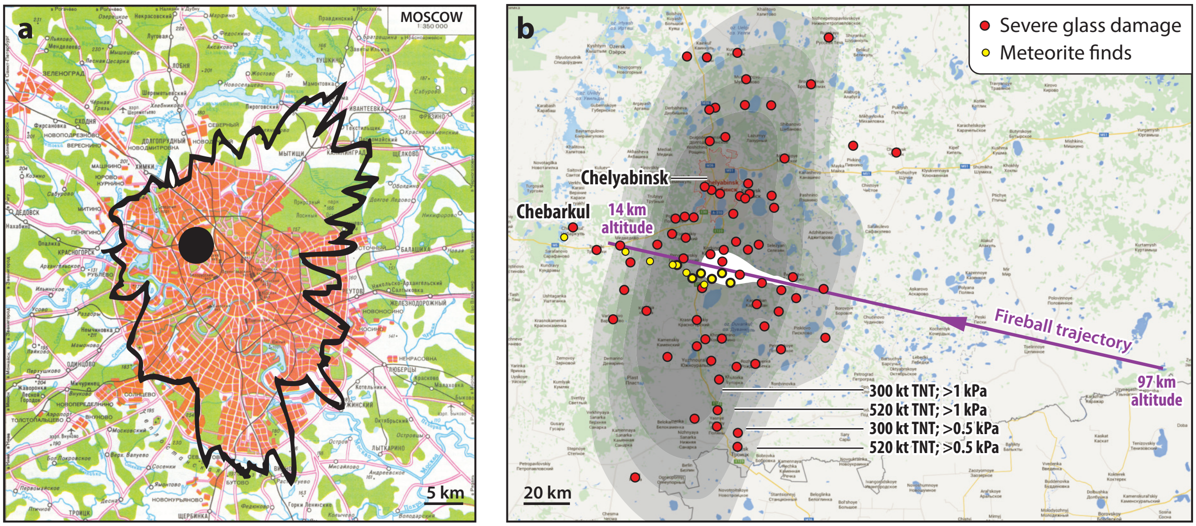

Figure 4

(*a*) The famous Tunguska butterfly overlying a map of Moscow; the black circle indicates the approximate epicenter. (*b*) Glass damage after the Chelyabinsk entry (*red circles*) and modeling results of overpressure on the surface (*gray contours*). Also shown are the locations of meteorite finds (*yellow circles*) and the ground-projected fireball trajectory (*purple line*), moving right to left from 97 to 14 km in altitude. The white area corresponds to the brightest bolide. Panel *b* adapted from Popova et al. (2013) with permission from AAAS. The damage (tree fall) observed after the Tunguska event was much stronger than damage (broken glass) observed after the Chelyabinsk event. Glass damage may have occurred up to 600 km from the epicenter after the Tunguska event, though evidence for this finding is not well supported.

spherical explosion at an altitude of about 35 km. Although some witnesses reported feeling heat emitted by the bolide, fires did not occur because of the high altitude of the explosion and its lower energy (relative to that of the Tunguska event). Minor disturbances in the ionosphere were registered, but electronic communications were not interrupted.

4.2. Plume Versus Smoke Train

The Chelyabinsk meteoroid was too small and its trajectory was too shallow to produce a plume. Instead, a dusty train was observed in the skies above the Ural Mountains for a period of at least half an hour. It rose very little, billowing and creating wavy structures in the process due to the development of turbulence and instabilities. It also split into two clearly separated trains because of buoyancy and the formation of two symmetrical cylindrical vortices (Brown et al. 2013, Artemieva & Shuvalov 2014) (**Figure 5**). The total mass of dust within the smoke train was probably ~25% of the preatmospheric meteoroid mass, similar to many other observed falls (Popova et al. 2013). It might also have been much larger, as fewer meteorites were recovered from the surface (Borovička et al. 2013). The leftovers of this train were observed in the upper atmosphere for the next three months by US and Japanese satellite sensors (Gorkavyi et al. 2013). Modeling results (Artemieva & Shuvalov 2014) have shown that, to form an atmospheric plume, the Chelyabinsk airburst would have required a meteoroid with eight times as much energy (i.e., twice the diameter) and a steeper impact angle (~45°).

5. AIRBURSTS AND IMPACT HAZARD

Environmental effects caused by airbursts are not as dramatic as those that follow large impact events that lead to mass extinctions (Toon et al. 1997). However, if an airburst similar to the Tunguska event occurred above a large city (such as Moscow or London), that city would suffer serious damage from the blast (**Figure 4*a***). An order-of-magnitude smaller airburst was able to destroy fragile structures in a densely populated area near Chelyabinsk. The heat pulse of a Tunguska-like impact could also ignite the surface (even during the Chelyabinsk entry, people felt a short heat pulse). Both shock and heat pulses become much more dangerous if they occur near vulnerable points in modern civilization, such as chemical or nuclear power plants, dams, and military facilities. In those cases, the consequences could be much more complicated and would not be directly related to the energy released.

Boslough & Crawford (1997) claimed that any small object, even a few meters in diameter, could create a rising plume and, hence, expel lower atmospheric gas and impactor materials with high velocity into satellite orbits (hundreds of kilometers above Earth's surface). Fortunately, these predictions were not quite correct—the atmospheric wake is highly turbulent, hot gases within the wake tend to mix with surrounding cold atmosphere, and narrow wakes (created by bodies 1–3 m in diameter) disappear quickly (Shuvalov 1999a). Also, if the entry trajectory is very shallow (as in the case of Chelyabinsk), the pressure gradient along the wake is not high enough to accelerate gases to high speeds. However, even minor impact-induced disturbances in the ionosphere could interrupt global communications, which are of extreme importance in emergency situations.

Both passage through the atmosphere and final fragmentation and deceleration of an asteroid would produce an enormous amount of nitric oxide (NO) via thermochemical reactions of N_2 and O_2 due to the high temperatures reached in shocked air. According to Zahnle (1990), a Tunguska-like impact yielded 7.5×10^{33} NO molecules, equivalent to 0.4 Tg nitric oxide. Curci et al. (2004) used a 3D chemistry and transport model of the global troposphere to determine that much of the NO forms nitric acid that deposits downwind of the blast site within the first month, with no severe damage to the ecosystem caused by acid rain.

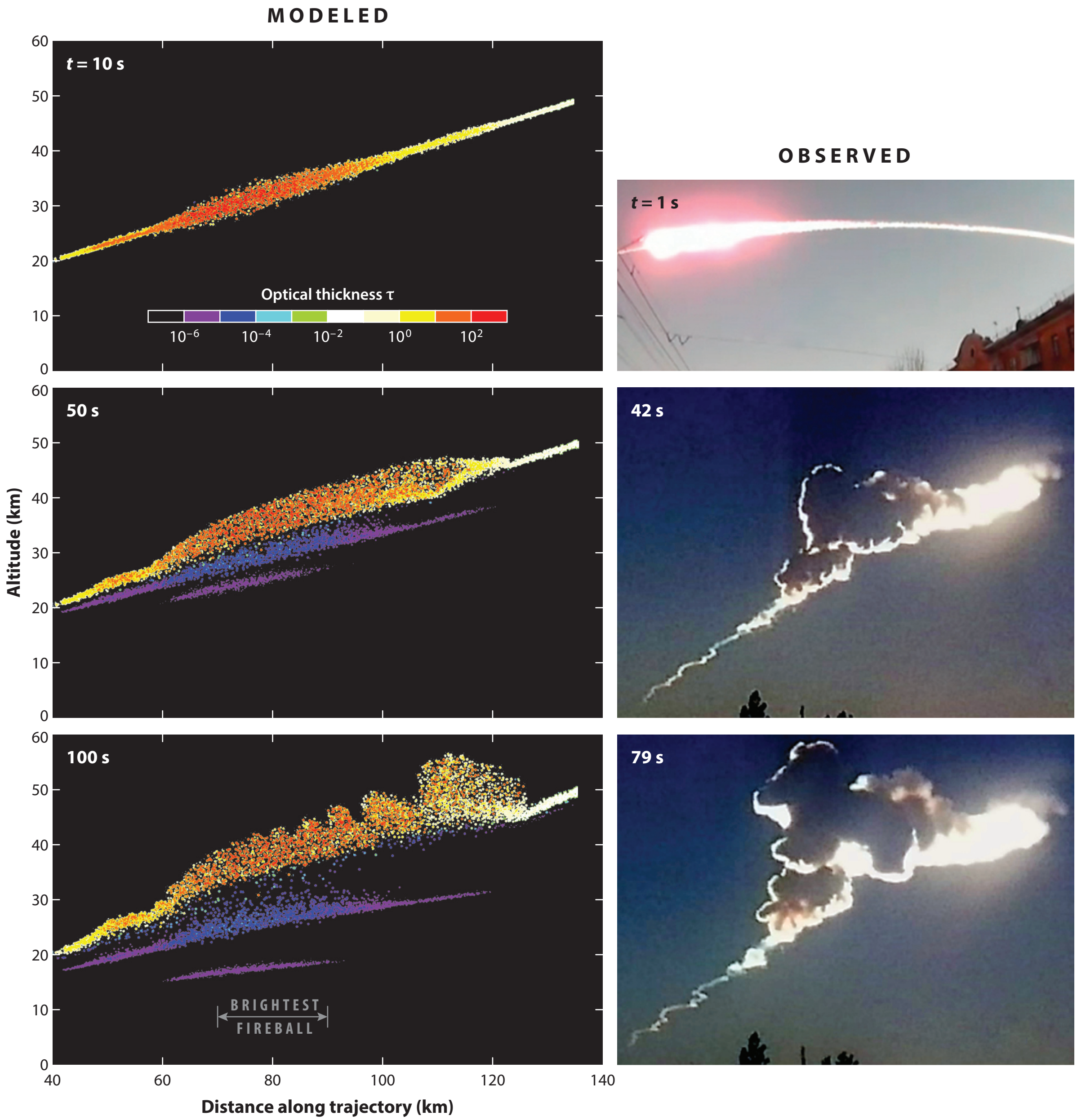

Figure 5

Modeled (*left*) and observed (*right*) smoke train left by the Chelyabinsk meteoroid. The point (0, 0) where distance and altitude are both equal to zero corresponds to the impact site of the largest fragment. Colors on the left correspond to the train optical thickness, τ; objects visible in atmosphere by the naked eye have $\tau > 0.01$. Vertical separation of the modeled train happens due to the presence of large particles within the train. These so-called duplets are essentially invisible. Panels on the right are modified from Gorkavyi et al. (2013) with permission from Wiley: top right panel, video by Sergei Zhabin; middle and bottom right panels, photos by Sergei Vladelschikov.

An overlooked hazard of small airbursts nowadays is the reaction of people who are not familiar with the specifics of such events. It is likely that some of the Chelyabinsk injuries could have been avoided if witnesses of the bright flash had sought cover and moved away from, rather than toward, windows broken by the ensuing blast. In this regard, it is important to improve public education about meteoroids and their interaction with the atmosphere as well as simple rules about appropriate responses. Those living in seismically active areas are well aware of earthquake hazards and know what actions to take in an emergency. Unlike an earthquake, a meteoroid impact may happen at any time, anywhere on Earth, making global education imperative. In addition, to avoid panic, local authorities must work together with emergency agencies to analyze and react to airburst situations as quickly as possible and to inform people using all available media, including cell phones and social media. The 1.5-h delay in providing information after the Chelyabinsk event is absolutely unacceptable.

The number of bodies of a given size that have impacted Earth over the last 3.9 billion years has been estimated, on the one hand, by combining the observed record of lunar impact craters with the absolute ages of a few impact structures deduced from absolute ages of lunar samples. On the other hand, telescopic observational surveys of small bodies orbiting the Sun, and associated dynamical models, have constrained the current number of possible impactors in hazardous, near-Earth orbits as a function of size. Such objects are known as near-Earth objects. As of the beginning of 2011, approximately 85% of near-Earth objects larger than 1 km in diameter had been discovered. Smaller bodies are much more abundant between near-Earth objects, and it was generally agreed that Tunguska-like impacts could occur at intervals of 100–10,000 years (Brown et al. 2002, Bland & Artemieva 2003). Brown et al. (2013) claimed that the impact rate on Earth of objects with diameters of 15–30 m is an order of magnitude larger. Although this discrepancy may be attributable to small-number statistics, the Chelyabinsk event tends to support a higher rate. At the same time, astronomical identification of small bodies is much less successful, because such objects are too small to be detected in space by modern telescopes. The only example of a successful prediction was the asteroid 2008 TC_3, which was found by accident one day prior to its encounter with Earth and was later recovered in Sudan as the Almahata Sitta meteorite (Jenniskens et al. 2009). Can scientists estimate the area at risk and the degree of damage for future impacts? The answer is quite uncertain. If we somehow come to know the trajectory, size, and composition (iron or stony) of a body, physicists would be able to predict its behavior—whether it will be fragmented and vaporized in the atmosphere or will reach the surface at a high enough velocity to produce an impact crater. They would also be able to estimate the impact site and the affected area with reasonable accuracy (Collins et al. 2005, Shuvalov et al. 2013). However, there is no way to collect crucial data about impactor properties (strength and density in particular) from telescopic observations.

6. CONCLUSIONS

The 1908 Tunguska event remained enigmatic for at least 80 years. The spectacular demise of Comet Shoemaker-Levy 9 in 1994 was the first atmospheric entry caught in the act, and it boosted our physical understanding of meteoroid-atmosphere interactions. Finally, the flight of the Chelyabinsk meteoroid in 2013 was a brilliant confirmation of our understanding of atmospheric and ground effects during medium-sized (tens of meters in diameter) meteoroid impacts. As this review summarizes, much of the observational data can be explained and are fully consistent with recent computational models. All airburst effects are defined mainly by impactor energy and entry angle. Early estimates (Ben-Menahem 1975) and models (Korobeinikov et al. 1998) of the 20 Mt TNT Tunguska event are still in good agreement with recent 3D models (Boslough & Crawford

1997; Shuvalov & Artemieva 2002; Artemieva & Shuvalov 2007, 2010). The total energy of the event is not well defined and may have been be 3–4 times lower (Boslough & Crawford 2008) if a specific impact scenario took place. Environmental effects of airbursts are usually minor. However, modern civilization could be extremely vulnerable even to small disturbances that recur on a decadal timescale and are difficult to predict. Prior education and adequate and timely information are key to avoiding panic if an impact occurs in a densely populated area.

The type of the Tunguska object cannot be defined without geochemical analysis of its material, which has not been found so far. Theoretical estimates show that the average concentration of its widely dispersed material is comparable to the annual flux of cosmic spherules onto Earth. The best chance to find Tunguska-related extraterrestrial materials is in areas with precise stratigraphic records (glaciers in Greenland and Iceland as well as sediments in Lake Baikal may be the best candidates).

SUMMARY POINTS

1. All observed Tunguska-related effects previously considered enigmatic are consistent with those of a typical airburst caused by a body 40–100 m in diameter entering Earth's atmosphere at cosmic velocity.
2. "Explosive" energy release in atmosphere is a consequence of catastrophic meteoroid fragmentation.
3. The butterfly tree fall pattern results from interaction between the surface and atmospheric shock waves generated by the impactor's oblique trajectory; the same waves caused earthquakes that were described by eyewitnesses and registered by local seismic stations.
4. The absence of meteorites on the surface is related to intense evaporation of a large (and therefore fragmented in the lower atmosphere) impactor during entry, entrainment of impactor leftovers into the impact plume, and worldwide dispersion of these products; the type of the Tunguska object cannot be defined without geochemical analysis of its material, which has not been found so far.
5. White nights in Europe may be explained by the presence of intense PMCs made from water lifted within the plume from the lower to the upper atmosphere; disturbances of Earth's magnetic field are related to long-lasting plume oscillations in the upper atmosphere and ionization in the ionospheric E layer.
6. The Chelyabinsk event is a little brother of the Tunguska event, but damage to infrastructure and related injuries were nonetheless quite impressive.
7. Small impacts cannot be predicted in advance; Earth's atmosphere decreases the risk of such impacts, though not to a negligible level.

FUTURE ISSUES

1. The total recovered mass of Chelyabinsk meteorites is ∼2 t, which is less than 0.02% of the meteoroid's preatmospheric mass. As energy (and hence mass) estimates derived from various sources are consistent, ablation of large bodies during atmospheric entry is more intense than traditionally predicted.

2. Current astronomical instruments are not able to detect small (<100 m) asteroids. Such "invisible" objects are certainly numerous and present a substantial impact hazard to densely populated and technically advanced yet fragile areas of Earth. Amateur astronomers can certainly help to provide prior warning.
3. Scientists have to spend some of their precious time to educate the public and to train younger generations in astronomy, including the specifics of small cosmic objects and the consequences of their collision with Earth.

DISCLOSURE STATEMENT

The authors are not aware of any affiliations, memberships, funding, or financial holdings that might be perceived as affecting the objectivity of this review.

ACKNOWLEDGMENTS

This study was partially supported by the Russian Science Foundation (grant 16-17-00107).

LITERATURE CITED

Alvarez LW, Alvarez W, Asaro F, Michel HV. 1980. Extraterrestrial cause for the Cretaceous-Tertiary extinction. *Science* 208:1095–108

Artemieva NA, Shuvalov VV. 2001. Motion of a fragmented meteoroid through the planetary atmosphere. *J. Geophys. Res.* 106(E2):3297–310

Artemieva NA, Shuvalov VV. 2007. 3D effects of Tunguska event on the ground and in atmosphere. *Lunar Planet. Sci. Conf. Abstr.* 38:1537

Artemieva NA, Shuvalov VV. 2010. Tunguska explosion—final remarks. *Lunar Planet. Sci. Conf. Abstr.* 41:1268

Artemieva NA, Shuvalov VV. 2014. *The smoke train of the Chelyabinsk meteoroid*. Presented at the 77th Annual Meteoritical Society Meeting, Sept. 7–12, Casablanca, Moroc., Abstr. 5113

Barringer DM. 1909. *Meteor Crater* (*Formerly Called Coon Mountain or Coon Butte*), *in Northern Central Arizona*. Princeton, NJ: privately printed

Ben-Menahem A. 1975. Source parameters of the Siberian explosion on June 30, 1908, from analysis and synthesis of signals at four stations. *Phys. Earth Planet. Inter.* 11:1–35

Bland PA, Artemieva NA. 2003. Efficient disruption of small asteroids by Earth's atmosphere. *Nature* 424:288–91

Borovička J, Spurný P, Brown P, Wiegert P, Kalenda P, et al. 2013. The trajectory, structure and origin of the Chelyabinsk asteroidal impactor. *Nature* 503:235–37

Borovička J, Spurný P, Koten P. 2007. Atmospheric deceleration and light curves of Draconid meteors and implications for the structure of cometary dust. *Astron. Astrophys.* 473:661–72

Boslough MBE, Crawford DA. 1997. Shoemaker-Levy 9 and plume-forming collisions on Earth. *Ann. N.Y. Acad. Sci.* 822:236–82

Boslough MBE, Crawford DA. 2008. Low-altitude airbursts and the impact threat. *Int. J. Impact Eng.* 35:1441–48

Boslough MBE, Crawford DA, Robinson AC, Trucano TG. 1994. Mass and penetration depth of Shoemaker-Levy 9 fragments from time-resolved photometry. *Geophys. Res. Lett.* 21:1555–58

Bronshten VA. 1999. The nature of the Tunguska meteorite. *Meteorit. Planet. Sci.* 34:723–28

Brown PG, Assink JD, Astiz L, Blaauw R, Boslough MB, et al. 2013. A 500-kiloton airburst over Chelyabinsk and an enhanced hazard from small impactors. *Nature* 503:238–41

Brown PG, Spalding RE, ReVelle DO, Tagliaferri E, Worden SP. 2002. The flux of small near-Earth objects colliding with the Earth. *Nature* 420:294–96

Carlson RW, Weissman PR, Segura M, Hui J, Smythe WD, et al. 1995. Galileo infrared observations of the Shoemaker-Levy 9 G impact fireball: a preliminary report. *Geophys. Res. Lett.* 22:1557–60
Chushkin PI, Sharipov AK. 1990. Large meteor body ablation by radiative heating. *Zh. Vychisl. Mat. Mat. Fiz.* 30:1815–26 (in Russian)
Chyba CF, Thomas PJ, Zahnle KJ. 1993. The 1908 Tunguska explosion: atmospheric disruption of a stony asteroid. *Nature* 361:40–44
Collins GS, Melosh HJ, Markus RA. 2005. Earth Impact Effects Program: a web-based computer program for calculating the regional environmental consequences of a meteoroid impact on Earth. *Meteorit. Planet. Sci.* 40:817–40
Crawford DA. 1997. Comet Shoemaker-Levy 9 fragment size estimates: How big was the parent body? *Ann. N.Y. Acad. Sci.* 822:155–73
Crawford DA, Boslough MBE, Trucano TG, Robinson AC. 1994. The impact of comet Shoemaker-Levy 9 on Jupiter. *Shock Waves* 4:47–50
Curci G, Visconti G, Jacob DJ, Evans MJ. 2004. Tropospheric fate of Tunguska generated nitrogen oxides. *Geophys. Res. Lett.* 31:L06123
Glasstone S, Dolan PJ. 1977. *The Effects of Nuclear Weapons*. Washington, DC: US Dep. Defense and US Energy Res. Dev. Admin. 3rd ed.
Gorkavyi N, Rault DF, Newman PA, Silva AM, Dudorov AE. 2013. New stratospheric dust belt due to the Chelyabinsk bolide. *Geophys. Res. Lett.* 40:4728–33
Grigorian SS. 1980. Motion and destruction of meteors in planetary atmospheres. *Cosmic Res.* 17:724–40
Hammel HB, Beebe RF, Ingersoll AP, Orton GS, Mills JR, et al. 1995. HST imaging of atmospheric phenomena created by the impact of comet Shoemaker-Levy 9. *Science* 267:1288–96
Harris AW. 2002. A new estimate of the population of small NEAs. *Bull. Am. Astron. Soc.* 34:835
Hills JG, Goda MP. 1993. The fragmentation of small asteroids in the atmosphere. *Astron. J.* 105:1114–44
Hou QL, Kolesnikov EM, Xie LW, Zhou MF, Sun M, Kolesnikova NV. 2000. Discovery of probable Tunguska cosmic body material: anomalies of platinum group elements and rare-earth elements in peat near the explosion site. *Planet. Space Sci.* 48:1447–55
Jenniskens P, Shaddad MH, Numan D, Elsir S, Kudoda AM, et al. 2009. The impact and recovery of asteroid 2008 TC_3. *Nature* 458:485–88
Kelley MC, Seyler CE, Larsen MF. 2009. Two-dimensional turbulence, space shuttle plume transport in the thermosphere, and a possible relation to the Great Siberian Impact Event. *Geophys. Res. Lett.* 36:L14103
Korobeinikov VP, Shurshalov LV, Vlasov VL, Semenov IV. 1998. Complex modelling of the Tunguska catastrophe. *Planet. Space Sci.* 46:231–44
Kovalev AT, Nemchinov IV, Shuvalov VV. 2006. Ionospheric and magnetospheric disturbances caused by impacts of small comets and asteroids. *Solar Syst. Res.* 40:57–67
Kulik L. 1927. On the fall of the Podkamennaya Tunguska meteorite in 1908, transl. L La Paz, G Wiens, 1935, in *Meteor Notes* 43:596–99 (from Russian)
Kulik LA. 1938. The meteorite of June 30, 1908, in Central Siberia. *Astron. Soc. Pac. Leafl.* 3:78–84
Kuzmicheva MY, Losseva TV. 2012. Simulations of the geomagnetic field disturbances caused by the Tunguska event 1908. *Lunar Planet. Sci. Conf. Abstr.* 43:2319
McGlaun JM, Thompson SL, Elrick MG. 1990. CTH: a three-dimensional shock waves physics code. *Int. J. Impact Eng.* 10:351–60
Merrill GP. 1908. The meteor crater of Canyon Diablo, Arizona—its history, origin and associated meteoritic irons. *Smithson. Misc. Collect.* 50:461–98
Nazarov MA, Korina MI, Kolesov GM, Vasil'ev N, Kolesnikov E. 1983. The Tunguska event: mineralogical and geochemical data. *Lunar Planet. Sci. Conf. Abstr.* 14:548–49
Nemtchinov IV, Shuvalov VV, Kosarev IB, Artemieva NA, Trubetskaya IA, et al. 1997. Assessment of comet Shoemaker-Levy 9 fragment sizes using light curves measured by Galileo spacecraft instruments. *Planet. Space Sci.* 45:311–26
Öpik EJ. 1916. A note on the meteoric theory of lunar craters. *Mirovedenie* 5:125–134 (in Russian)
Pasechnik IP. 1976. Evaluation of parameters of the Tunguska meteorite explosion by seismic and microbarographic data. In *Space Matter in the Earth*, pp. 25–54. Novosibirsk, Russ.: Nauka (in Russian)

Passey QR, Melosh HJ. 1980. Effects of atmospheric breakup on crater field formation. *Icarus* 42:211–33
Petrov GI, Stulov VP. 1976. Motion of large bodies in the atmospheres of planets. *Cosmic Res.* 13:525–31
Petrovic JJ. 2001. Mechanical properties of meteorites and their constituents. *J. Mater. Sci.* 36:1579–83
Pierazzo E, Vickery AM, Melosh HJ. 1997. A reevaluation of impact melt production. *Icarus* 127:408–23
Popova O, Borovička J, Hartmann WK, Spurný P, Gnos E, et al. 2011. Very low strengths of interplanetary meteoroids and small asteroids. *Meteorit. Planet. Sci.* 46:1525–50
Popova O, Jenniskens P, Emel'yanenko V, Kartashova A, Biryukov E, et al. 2013. Chelyabinsk airburst, damage assessment, meteorite recovery, and characterization. *Science* 342:1069–73
Shoemaker EM, Shoemaker CS, Levy DH. 1993. Collision of P/Shoemaker-Levy 9 with Jupiter. *Bull. Am. Astron. Soc.* 25:1042
Shuvalov VV. 1999a. Atmospheric plumes created by meteoroids impacting the Earth. *J. Geophys. Res.* 104(E3):5877–89
Shuvalov VV. 1999b. Multi-dimensional hydrodynamic code SOVA for interfacial flows: application to the thermal layer effect. *Shock Waves* 9:381–90
Shuvalov VV, Artemieva NA. 2002. Numerical modeling of Tunguska-like impacts. *Planet. Space Sci.* 50:181–92
Shuvalov VV, Svettsov VV, Trubetskaya IA. 2013. An estimate for the size of the area of damage on the Earth's surface after impacts of 10–300-m asteroids. *Solar Syst. Res.* 47:260–67
Shuvalov VV, Trubetskaya IA. 2007. Aerial bursts in the terrestrial atmosphere. *Solar Syst. Res.* 41:220–30
Stevens MH, Gumbel J, Englert CR, Grossmann KU, Rapp M, Hartogh P. 2003. Polar mesospheric clouds formed from space shuttle exhaust. *Geophys. Res. Lett.* 30:1546
Svetsov VV. 1996. Total ablation of the debris from the 1908 Tunguska explosion. *Nature* 383:697–99
Svetsov VV. 1998. Could the Tunguska debris survive the terminal flare? *Planet. Space Sci.* 46:261–68
Svetsov VV, Nemtchinov IV, Teterev AV. 1995. Disintegration of large meteoroids in Earth's atmosphere: theoretical models. *Icarus* 116:131–53
Svettsov VV. 2007. Estimates of the energy of surface waves from atmospheric explosions and the source parameters of the Tunguska event. *Izv. Phys. Solid Earth* 43:583–91
Thomas GE, McKay CP. 1985. On the mean particle size and water content of polar mesospheric clouds. *Planet. Space Sci.* 33:1209–24
Toon OB, Zahnle KJ, Morrison D, Turco RP, Covey C. 1997. Environmental perturbations caused by the impacts of asteroids and comets. *Rev. Geophys. Space Phys.* 35:41–78
Vasilyev NV. 1998. The Tunguska meteorite problem today. *Planet. Space Sci.* 46:129–50
Weaver HA, A'Hearn MF, Arpigny C, Boice DC, Feldman PD, et al. 1995. The Hubble Space Telescope (HST) observing campaign on Comet Shoemaker-Levy 9. *Science* 267:1282–88
Wegener A. 1921. The origin of lunar craters, transl. AMC Sengôr, 1975, in *Moon* 14:211–36 (from German)
Weibull W. 1951. A statistical distribution function of wide applicability. *J. Appl. Mech.* 18:140–47
Werner SC, Harris AW, Neukum G, Ivanov BA. 2002. The near-Earth asteroid size-frequency distribution: a snapshot of the lunar impactor size-frequency distribution. *Icarus* 156:287–90
Zahnle K. 1990. Atmospheric chemistry by large impacts. *Geol. Soc. Am. Spec. Pap.* 247:271–88
Zahnle K, MacLow MM. 1994. The collision of Jupiter and Comet Shoemaker-Levy 9. *Icarus* 108:1–17
Zotkin IT, Tsikulin MA. 1966. Simulation of the explosion of the Tungus meteorite. *Sov. Phys. Dokl.* 11:183–86

RELATED RESOURCES

Impact: Earth! A Web-based program to calculate the effects of impacts, including airbursts. The accuracy is not very high; numbers must be treated as averages, and each particular case requires special consideration. **http://impact.ese.ic.ac.uk/**

Near Earth Object Program. Information and recent news about near-Earth objects, provided by NASA. **http://neo.jpl.nasa.gov/**